DHPR activation underlies SR Ca^{2+} release induced by osmotic stress in isolated rat skeletal muscle fibers

James D. Pickering, Ed White, Adrian M. Duke, and Derek S. Steele

Institute of Membrane and Systems Biology, Faculty of Biological Sciences, University of Leeds, Leeds LS2 9JT, England, UK

Changes in skeletal muscle volume induce localized sarcoplasmic reticulum (SR) Ca^{2+} release (LCR) events, which are sustained for many minutes, suggesting a possible signaling role in plasticity or pathology. However, the mechanism by which cell volume influences SR Ca^{2+} release is uncertain. In the present study, rat flexor digitorum brevis fibers were superfused with isoosmotic Tyrode's solution before exposure to either hyperosmotic (404 mOsm) or hypoosmotic (254 mOsm) solutions, and the effects on cell volume, membrane potential (E_m), and intracellular Ca^{2+} ($[Ca^{2+}]_i$) were determined. To allow comparison with previous studies, solutions were made hyperosmotic by the addition of sugars or divalent cations, or they were made hypoosmotic by reducing $[NaCl]_o$. All hyperosmotic solutions induced a sustained decrease in cell volume, which was accompanied by membrane depolarization (by 14–18 mV; $n = 40$) and SR Ca^{2+} release. However, sugar solutions caused a global increase in $[Ca^{2+}]_i$, whereas solutions made hyperosmotic by the addition of divalent cations only induced LCR. Decreasing osmolarity induced an increase in cell volume and a negative shift in E_m (by 15.04 ± 1.85 mV; $n = 8$), whereas $[Ca^{2+}]_i$ was unaffected. However, on return to the isoosmotic solution, restoration of cell volume and E_m was associated with LCR. Both global and localized SR Ca^{2+} release were abolished by the dihydropyridine receptor inhibitor nifedipine by sustained depolarization of the sarcolemmal or by the addition of the ryanodine receptor 1 inhibitor tetracaine. Inhibitors of the Na-K-2Cl (NKCC) cotransporter markedly inhibited the depolarization associated with hyperosmotic shrinkage and the associated SR Ca^{2+} release. These findings suggest (1) that the depolarization that accompanies a decrease in cell volume is the primary event leading to SR Ca^{2+} release, and (2) that volume-dependent regulation of the NKCC cotransporter contributes to the observed changes in E_m. The differing effects of the osmotic agents can be explained by the screening of fixed charges by divalent ions.

INTRODUCTION

Skeletal muscle swells as a consequence of intense activity and gradually returns to its original volume after cessation of exercise (Sjogaard et al., 1985; Peeze Binkhorst et al., 1990; Watson et al., 1993; Raja et al., 2006). Swelling occurs due to an accumulation of metabolites within the cytosol and a consequent increase in osmolarity, which drives the entry of water from the extracellular space (Nagesser et al., 1992; Sejersted and Sjogaard, 2000; Lannergren et al., 2002; Raja et al., 2006).

Recent studies have sought to establish the functional consequences of cell volume changes in mammalian skeletal muscle; e.g., in mouse flexor digitorum brevis (FDB) fibers, transient swelling induced by exposure to hypoosmotic Tyrode's solution ([NaCl] decreased: 140 to 70 mM) induced localized SR Ca^{2+} release (LCR), which was sustained for several minutes (Wang et al., 2005; Weisleder et al., 2006; Martins et al., 2008; Weisleder and Ma, 2008). This form of LCR occurred mostly at the cell periphery and was reported to involve both Ca^{2+} sparks and events of longer duration, termed "Ca^{2+} bursts" (Weisleder and Ma, 2006). Interestingly, the initiation of LCR actually coincided with the restoration of cell volume after the reintroduction of the isoosmotic solution (Wang et al., 2005; Martins et al., 2008). Furthermore, LCR could be triggered by an immediate decrease in cell volume after exposure to a hyperosmotic solution ($[CaCl_2]$ increased: 2.5 to 50 mM) (Weisleder and Ma, 2006). These findings suggest that LCR is linked mechanistically to decreasing cell volume and occurs whether or not this is preceded by swelling.

In further experiments, LCR was found to be initiated by intense exercise and modified by age or disease, suggesting a potentially important signaling role in muscle plasticity or pathology (Wang et al., 2005; Weisleder et al., 2006; Teichmann et al., 2008; Weisleder and Ma, 2008). However, some aspects of these recent findings differ from earlier work; e.g., in rat skeletal muscle, a decrease in cell volume induced by exposure to a hyperosmotic sucrose solution caused a sustained contracture (Clausen et al., 1979; Bruton, 1989), which likely reflects a larger,

Correspondence to Derek S. Steele: d.steele@leeds.ac.uk

Abbreviations used in this paper: $[Ca^{2+}]_i$, intracellular Ca^{2+}; CSA, cross-sectional area; DHPR, dihydropyridine receptor; E_m, membrane potential; FDB, flexor digitorum brevis; FDHM, full duration half maximum; LCR, localized SR Ca^{2+} release; NKCC, Na-K-2Cl; SAC, stretch-activated Ca^{2+} channel.

The Rockefeller University Press $30.00
J. Gen. Physiol. Vol. 133 No. 5 511–524
www.jgp.org/cgi/doi/10.1085/jgp.200910191

global increase in intracellular Ca^{2+} ($[Ca^{2+}]_i$). In amphibian fibers, hyperosmotic sugar solutions induced a global rise in $[Ca^{2+}]_i$, which took the form of a propagated Ca^{2+} wave (Chawla et al., 2001). As these experimental protocols suggest that the response to a given change in cell volume is influenced markedly by the choice of osmotic agent (i.e., sugars vs. ions), it remains uncertain which form of SR Ca^{2+} release is physiologically relevant.

The mechanism by which decreasing cell volume leads to SR Ca^{2+} release is also uncertain; e.g., it has been suggested that the initiation of LCR may involve structural changes at the triadic junction (Wang et al., 2005), mechanical deformation of the membrane (Teichmann et al., 2008), or increased production of reactive oxygen species (Isaeva et al., 2005; Martins et al., 2008). However, another possibility not yet considered is that changes in cell volume may influence membrane potential (E_m), thereby altering RYR1 function via dihydropyridine receptor (DHPR) activation. Membrane depolarization can occur in skeletal muscle (van Mil et al., 1997; Geukes Foppen, 2004) and other cell types (Wang and Wondergem, 1992; Hattori and Wang, 2006) after exposure to hyperosmotic solutions. This is believed to involve volume-dependent activation of the Na-K-2Cl (NKCC) cotransporter and consequent effects of $[Cl^-]_i$ (van Mil et al., 1997; Ferenczi et al., 2004; Geukes Foppen, 2004; Hattori and Wang, 2006). However, it is not yet known whether volume-dependent effects on E_m can induce SR Ca^{2+} release in mammalian skeletal muscle.

In the present study, the effects of cell volume on E_m and $[Ca^{2+}]_i$ were characterized in rat FDB fibers. To enable direct comparison with previous studies, hyperosmotic solutions were prepared either by the addition of sugars or divalent cations to Tyrode's solution. Alternatively, cells were transiently exposed to solutions made hypoosmotic by a reduction in $[NaCl]_o$. The data show that a decrease in cell volume is consistently associated with a positive shift in E_m, which is sufficient to trigger SR Ca^{2+} release. The mechanism underlying volume-dependent changes in E_m, differences between osmotic agents, and the possible physiological relevance of these effects are discussed.

MATERIALS AND METHODS

Muscle fiber isolation and stimulation

Male Wistar rats (250–300 g) were killed in accordance with Schedule 1 procedures of the Home Office Guidance on the Operation of Animals (Scientific Procedures) Act of 1986, UK. Experiments also conformed to the Guide for the Care and Use of Laboratory Animals (1996. National Academy of Sciences, Washington D.C.).

FDB muscles were dissected in a modified Tyrode's solution (see below) and incubated in 0.9 mg/ml collagenase (type 1; Worthington Biochemical) at 37°C for 2 h. Muscle bundles were then washed in Tyrode's solution containing pluronic-F68 (800 ng/1 ml) for trituration into a series of test tubes and used within 4 h. Isolated fibers were allowed to settle in bath with a coverslip base and superfused with isoosmotic Tyrode's solution. Only cells that adhered to the coverslip strongly enough to prevent them from being washed away by the solution flow were studied. Before each protocol, cells were field stimulated at 10-s intervals using a square wave voltage pulse (1.2× threshold, delivered via platinum electrodes) to assess fiber viability. Only fibers producing strong twitch responses were used. All protocols were performed at 20–22°C.

Solutions

All chemicals were purchased from Sigma-Aldrich unless otherwise stated. The isoosmotic Tyrode's solution contained (in mM): 140.3 NaCl, 2.48 KCl, 1 $CaCl_2$, 1 $MgCl_2$, 5 HEPES, 5 glucose, and 5 Na pyruvate, with a total Cl^- concentration of 144.78 (298 mOsm). For experiments looking at $[Cl^-]_e$ withdrawal, a similar solution was generated using sulfate as the extracellular anion. This was (in mM): 70 Na_2SO_4, 1 K_2SO_4, 1 $MgSO_4$, 1 $CaSO_4$, 5 HEPES, 5 glucose, and 5 Na pyruvate. To produce solutions with lowered $[Cl^-]_e$, appropriate amounts of these solutions were mixed. The pH was adjusted to 7.2 with NaOH, and osmolarity was measured using an osmometer (LH Roebling). Hyperosmotic (~404 mOsm) solutions were prepared by the addition of either 50 mM $CaCl_2$, 50 mM $MgCl_2$, 120 mM sucrose, or 125 mM mannitol. A hypoosmotic solution (254 mOsm) was prepared by reducing NaCl from 140.3 to 70 mM as described previously (Wang et al., 2005). The high K^+ solution contained all of the above chemicals but had KCl increased to 100 mM and NaCl reduced to 20 mM. Stocks of 1 mM fura-2 AM (Biotium Inc.), 1 mM fluo-4 AM (Invitrogen), 1 mM tetracaine, 100 µM nifedipine (MP Biomedicals), 100 µM 9-AC (Alfa Aesar), 200 µM furosemide, or 1 mM bumetanide were dissolved in DMSO. The final level of DMSO was within the range of 0.1 to 0.5%. The addition of 0.5% DMSO was not found to influence E_m or $[Ca^{2+}]_i$ under the conditions used in this study.

Nifedipine block of DHPR-mediated SR Ca^{2+} release

Before exposure to nifedipine, four to five twitch responses (monitored as fura-2 or fluo-3 fluorescence transients) to field stimulation were initiated to establish fiber viability. Nifedipine was then introduced and the fibers were stimulated with single-twitch responses at ~30-s intervals, allowing for the progressive inhibition of DHPR activation to be monitored. 10-min exposure to 100 µM nifedipine was sufficient to abolish SR Ca^{2+} release in all fibers.

Fiber cross-sectional area (CSA) as an index of volume

In experiments designed to assess the effects of osmolarity on cell volume, fibers were initially superfused with a control isoosmotic solution before changing to either a hyperosmotic or hypoosmotic solution (see above). Videos were acquired with a QImaging Fast 1394 CCD camera (Cairn Research) mounted on the microscope side port. Images were then viewed and analyzed using Image Pro-Plus (Version 5.1; Media Cybernetics). CSA was calculated by measuring the width of the fiber and applying the equation $CSA = \pi(D/2)^2$, where D is the width, assuming a circular fiber cross section. The calculated CSA was used as an index of cell volume (Wang et al., 2005). The use of CSA as an index of cell function assumes that the fibers are approximately cylindrical and that changes in CSA are similar along the length of each fiber. CSA was generally measured close to the center of the cell and furthest away from the fiber ends, which were more prone to movement due to reduced contact with the coverslip. In all figures, CSA is expressed relative to the control value measured in isoosmotic Tyrode's solution.

Measurement of E_m

Sharp microelectrodes (resistance of 60–90 MΩ) filled with 3 M KCl were used to measure E_m relative to an Ag/AgCl reference electrode. To avoid junction potentials in experiments where the

$[Cl^-]_o$ was manipulated, the Ag/AgCl reference (bath) electrode was replaced by free-flowing KCl-Ag/AgCl reference electrode comprising a second micropipette with a broken tip to allow free access of the solution to the perfusate. The micropipette was filled with 3 M KCl and contained a Ag/AgCl electrode, which was positioned downstream of the preparation in the exit tract of the bath.

Microelectrodes were prepared using a P-30 Micropipette Puller (Sutter Instrument Co.). The microelectrodes were connected to an Axoclamp 2B amplifier via a HS-2A headstage. Electrophysiological data were sampled at 1.6 KHz. In some experiments, E_m and spatially averaged $[Ca^{2+}]_i$ were measured simultaneously (see below).

The resting E_m measured using sharp microelectrodes was found to be -60.1 ± 2.91, $n = 67$, which is consistent with previous findings in FDB fibers (Bekoff and Betz, 1977a,b; Westerblad and Allen, 1996). In control experiments, a similar value (-61.33 ± 1.37 mV; $n = 6$) was obtained from surface fibers of freshly dissected whole FDB muscles superfused with Tyrode's solution (not depicted). In contrast, the resting E_m recorded under the same conditions from the surface fibers of whole rat soleus or extensor digitorum longus muscles was -74.03 ± 2.1 mV ($n = 5$) and -73.03 ± 2 ($n = 6$). Thus, the lower E_m of FDB fibers does not reflect damage incurred during muscle dissection or subsequent cell isolation (see Discussion).

Measurement of spatially averaged $[Ca^{2+}]_i$

For spatially averaged $[Ca^{2+}]_i$ measurements, freshly isolated FDB muscle fibers were incubated in an isoosmotic Tyrode's solution containing 5 μM fura-2 AM for 45 min at 20–22°C. Cells were then resuspended for 20 min in fresh isoosmotic Tyrode's solution before proceeding with the experiment. The preparation was alternately illuminated with UV light (wavelengths of 340 and 380 nm, 50 Hz) using a spinning wheel spectrophotometer (Cairn Research). The average $[Ca^{2+}]_i$ within the visual field containing the preparation was indicated by the ratio of light intensities emitted at >510 nm. Light emitted from areas not occupied by the muscle image was excluded using a variable rectangular diaphragm positioned on the side port of the microscope. Records of spatially averaged $[Ca^{2+}]_i$ are presented as the 340:380 fluorescence ratio.

Confocal microscopy

Confocal microscopy was performed using a Bio-Rad Laboratories Cellmap system attached to the side port of a Nikon TE3000 microscope (excitation 488 nm; Plan Fluor Nikon objective, X40; oil immersion). Isolated FDB muscle fibers were loaded with 5 μM fluo-4 AM for 30 min at 20–22°C. Cells were then incubated in a control isoosmotic solution for 20 min before commencing measurements. To obtain information about the effects of osmolarity on the frequency of LCR events, confocal images were obtained in x-y mode at 1-s intervals. This approach prevented any detectable cell damage or dye bleaching associated with laser exposure, allowing data to be collected for ≥5 min. Alternatively, the time course and spatial characteristic LCR events were determined by scanning cells continuously in line-scan mode, but for briefer periods (≤60 s). Data were analyzed using ImageJ (National Institutes of Health; http://rsbweb.nih.gov/ij/) and Image Pro-Plus version 5.1 (Media Cybernetics). The automated detection of Ca^{2+} sparks and the measurement of temporal and spatial LCR properties were performed using the Sparkmaster plug-in for ImageJ, with the detection criteria set to 3.8; i.e., the threshold for the detection of events was 3.8 times the standard deviation of the background noise divided by the mean (Picht et al., 2007).

Statistical analysis

Cumulative data for spatially averaged $[Ca^{2+}]_i$ are shown as changes in fluorescence ratio units; E_m was analyzed at steady state during isoosmotic, hyperosmotic, and hypoosmotic superfusion. All cumulative data are represented as mean ± SEM, with the number of observations in parenthesis (n). Statistical significance was determined with one-way ANOVA. All analysis was performed using Origin software (Microcal).

RESULTS

Volume changes induced by hyperosmotic and hypoosmotic Tyrode's solution

Fig. 1 A shows x-y images of an isolated FDB fiber before, during, and after exposure to a hyperosmotic sucrose solution (top) and a corresponding record of CSA (bottom), an index of cell volume (see Materials and methods). A sustained decrease in CSA occurred on changing from the control isoosmotic (298 mOsm) solution to a hyperosmotic (404 mOsm) sucrose solution. This effect was reversed on reintroduction of the isoosmotic solution.

This protocol was used to compare the influence of solutions made hyperosmotic (404 mOsm) by the addition of various osmotic agents (sucrose, mannitol, $CaCl_2$, and $MgCl_2$) or hypoosmotic (254 mOsm) by a reduction in [NaCl] (Fig.1 B). In fibers exposed to the hypoosmotic solution, the normalized CSA increased to a maximum of 1.28 ± 0.04 ($n = 8$; $P < 0.001$) with a half-time of 38.71 ± 0.62 s. Solutions made hyperosmotic by the addition of sucrose, mannitol, $CaCl_2$, or $MgCl_2$ decreased CSA to $0.79 + 0.026$ ($n = 8$), 0.82 ± 0.023 ($n = 8$), 0.82 ± 0.025 ($n = 8$), and 0.81 ± 0.012 ($n = 8$), with half-times of 43.13 ± 1.18, 43.01 ± 1.31, and 42.01 ± 0.59 s, respectively. The steady-state change in CSA induced by the four hyperosmotic agents was not significantly different ($P > 0.05$; $n = 8$). In a group of control cells exposed to an isoosmotic solution throughout, there was no significant change in CSA ($P > 0.05$; $n = 5$).

Effects of hypoosmotic or hyperosmotic solutions on spatially averaged $[Ca^{2+}]_i$

The effects of exposure to hypoosmotic or hyperosmotic solutions on spatially averaged $[Ca^{2+}]_i$ were studied in fibers loaded with fura-2 AM. The introduction of a hypoosmotic Tyrode's solution had no significant effect on $[Ca^{2+}]_i$ ($n = 8$; $P > 0.05$). However, returning to the control isoosmotic solution was associated with a small but prolonged increase in resting $[Ca^{2+}]_i$ (Fig. 2 A). Exposure to hyperosmotic sucrose solution caused a more pronounced rise in $[Ca^{2+}]_i$, which peaked after ~1 min (Fig. 2 B, top left). In contrast, despite a comparable decrease in cell volume (Fig. 1), exposure to hyperosmotic $CaCl_2$ induced a much smaller increase in resting $[Ca^{2+}]_i$ (Fig. 2 B, bottom left). Further experiments were performed using mannitol or Mg^{2+} as osmotic agents. Hyperosmotic mannitol solution induced a robust rise in $[Ca^{2+}]_i$, although the transient was of smaller amplitude and slower to peak than that induced by sucrose

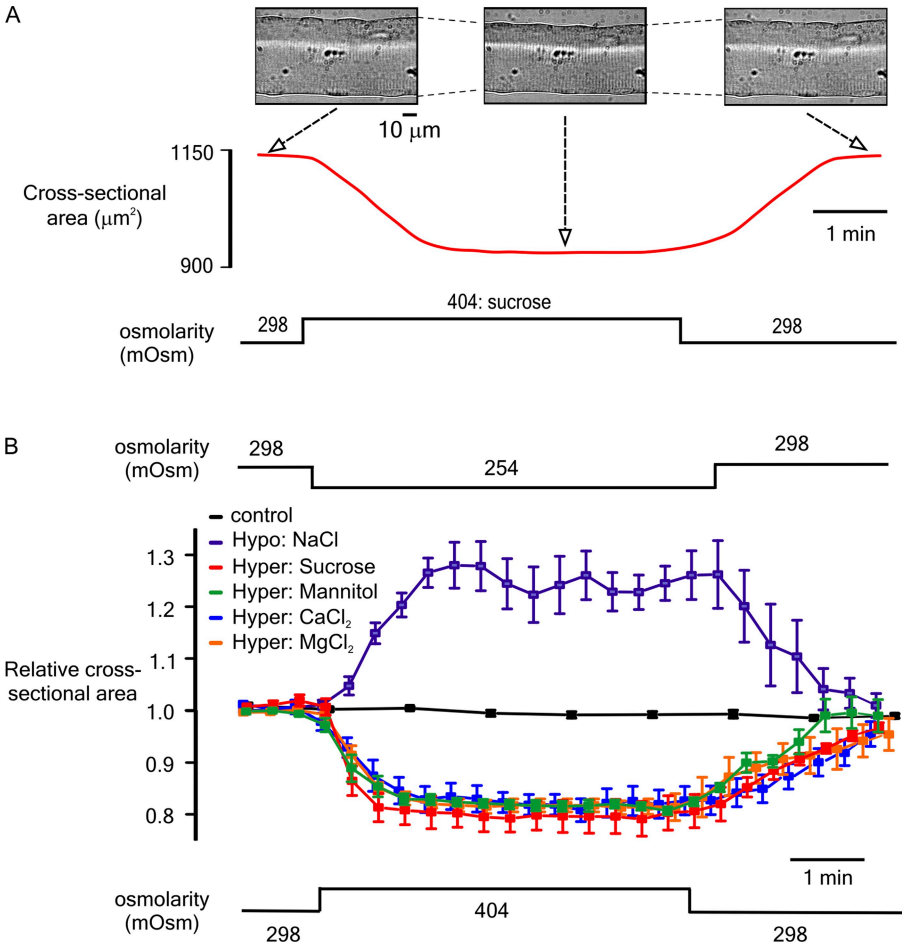

Figure 1. (A) Representative x-y images of an FDB muscle fiber before, during, and after exposure to a hyperosmotic sucrose solution (top) and a corresponding continuous record of CSA (bottom). (B) Cumulative data showing the relative change in CSA after transient exposure to a solution made hypoosmotic (254 mOsm) by decreasing [NaCl] or hyperosmotic (404 mOsm) by the addition of sucrose, mannitol, $CaCl_2$, or $MgCl_2$ as indicated. Also plotted are control data obtained during constant perfusion with an isoosmotic solution throughout. All data are presented as mean (± SEM). Steady-state changes in CSA induced by all four hyperosmotic agents were not significantly different ($P > 0.05$; $n = 8$). There was no significant change in CSA in control cells exposed to isoosmotic solutions throughout ($P > 0.05$; $n = 5$).

(Fig. 2 B, top right). As with $CaCl_2$, exposure to hyperosmotic $MgCl_2$ solution resulted in a small slow rise in resting $[Ca^{2+}]_i$ (Fig. 2 B, bottom right).

To establish the role of the SR in the response to a rapid increase in osmolarity, cells were exposed to hyperosmotic sucrose or $CaCl_2$ solutions in the presence of the RYR1 inhibitor tetracaine. As shown in Fig. 2 C (left), tetracaine markedly inhibited the rise in $[Ca^{2+}]_i$ after the introduction of a hyperosmotic sucrose solution. The amplitude of the already small response to hyperosmotic $CaCl_2$ solution was little affected by the presence of tetracaine (Fig. 2 C, right).

Cumulative data from these experiments is shown in Fig. 2 D. The amplitudes of the responses to hyperosmotic $CaCl_2$ or $MgCl_2$ were not significantly different from each other ($P > 0.05$; $n = 7$), but they were markedly smaller than those induced by either mannitol or sucrose ($P < 0.001$; $n = 8$). Unexpectedly, the response to mannitol was consistently slower to peak and smaller in amplitude than that induced by sucrose ($P < 0.01$; $n = 7$). In the presence of tetracaine, the response to hyperosmotic sucrose was markedly reduced by 88.5 ± 2.2% ($P < 0.001$; $n = 6$). The already small response to hyperosmotic $CaCl_2$ was not significantly affected by tetracaine ($P > 0.05$; $n = 7$).

Effects of hypoosmotic or hyperosmotic solutions on E_m

One possible explanation for the rise in $[Ca^{2+}]_i$ induced by hyperosmotic solutions is that the associated decrease in cell volume may result in sarcolemmal depolarization and subsequent DHPR activation (van Mil et al., 1997; Geukes Foppen, 2004). To investigate this possibility, E_m was measured during the initiation of SR Ca^{2+} release, triggered by a change in osmolarity.

Fig. 3 A shows simultaneous records of E_m (top) and $[Ca^{2+}]_i$ (bottom) before, during, and after the introduction of solutions made hyperosmotic by the addition of sucrose, $CaCl_2$, or mannitol, or made hypoosmotic by a reduction in [NaCl]. In these examples, hyperosmotic sucrose, mannitol, and $CaCl_2$ solutions induced membrane depolarizations of 14.5, 13.4, and 16.7 mV, respectively. In each case, E_m returned toward the control value on the reintroduction of the isoosmotic solution. In contrast, exposure to the hypoosmotic Tyrode's solution was associated with a hyperpolarization of 15 mV. Interestingly, the depolarization phase on returning to the control isoosmotic solution coincided with a small rise in resting $[Ca^{2+}]_i$ (see Figs. 2 A and 3 A).

Experiments were performed to establish whether the depolarization induced by exposure to hyperosmotic solutions is responsible for triggering the concomitant

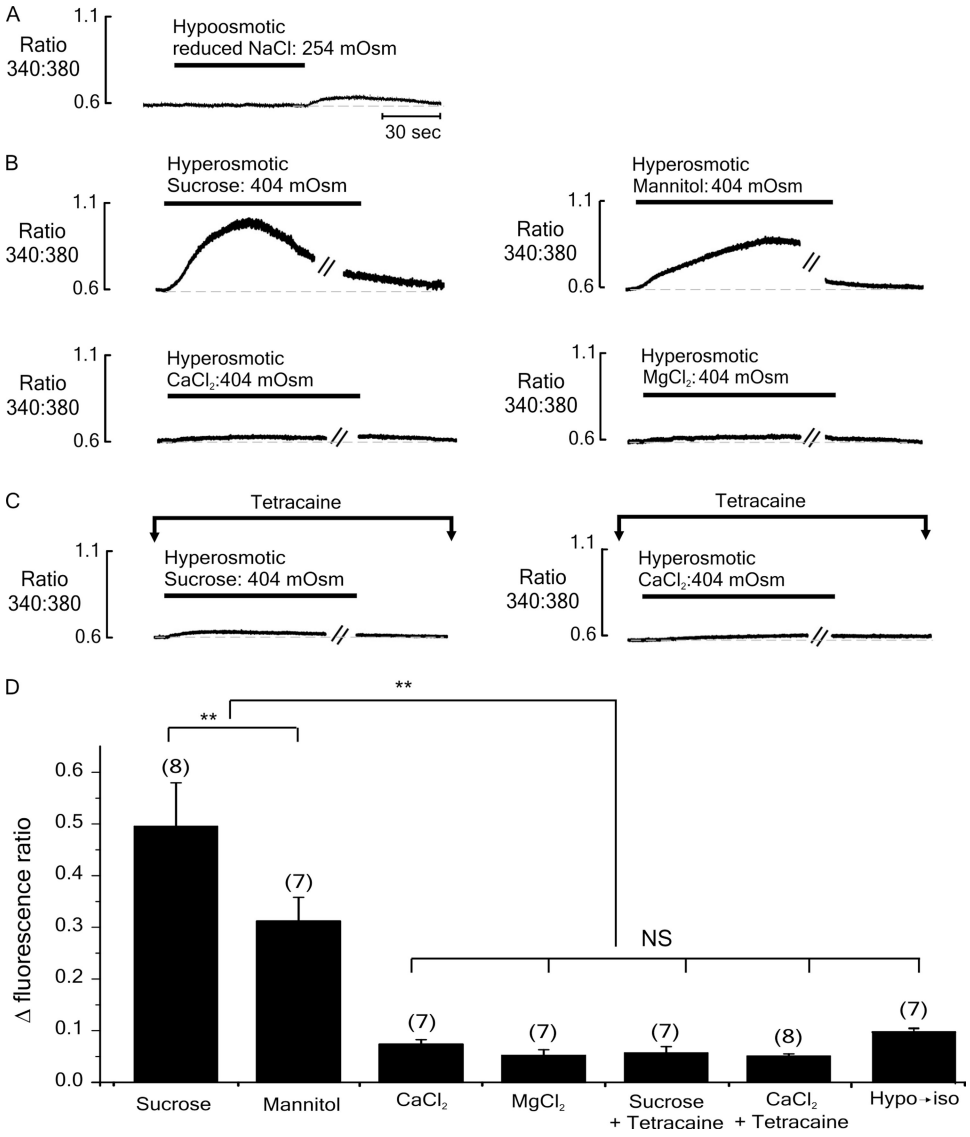

Figure 2. Typical records of $[Ca^{2+}]_i$ (expressed as the 340:380-nm fura-2 fluorescence ratio) from individual FDB fibers initially bathed in an isoosmotic (298 mOsm) solution. (A) Exposure to hypoosmotic (254 mOsm) solution for 2 min had no apparent effect on $[Ca^{2+}]_i$. However, the reintroduction of the control isoosmotic solution was associated with a small rise in resting $[Ca^{2+}]$i. (B) The introduction of hyperosmotic sucrose (top left) or mannitol (top right) solutions induced a long-lasting increase in resting $[Ca^{2+}]$. In contrast, the introduction of solutions made hyperosmotic (404 mOsm) by the addition of $CaCl_2$ (bottom left) or $MgCl_2$ (bottom right) induced a much smaller rise in resting $[Ca^{2+}]_i$. (C) In the presence of the RYR1 inhibitor tetracaine (1 mM), the response to hyperosmotic sucrose was markedly reduced (left). The response to hyperosmotic $CaCl_2$ solution also appeared smaller in the presence of tetracaine (right). (D) Accumulated data showing the relative change in fluorescence ratio with each protocol. Each bar represents the mean (± SEM), and the number of preparations is indicated in parentheses. Breaks in trace (−//−) represent 3.5 min. **, significantly different ($P < 0.05$); NS, not significantly different ($P > 0.05$).

rise in $[Ca^{2+}]_i$ (Fig. 3 B). Cells were exposed to DHPR inhibitor nifedipine (100 μM) for 10 min before the introduction of solutions made hyperosmotic by the addition of either sucrose or $CaCl_2$. In control experiments, exposure to 100 μM nifedipine for 10 min was sufficient to abolish the twitch response to field stimulation (not depicted). After exposure to nifedipine, the rise in $[Ca^{2+}]_i$ associated with the introduction of hyperosmotic sucrose or $CaCl_2$ solutions was barely detectable. In further experiments, substitution of 100 mM Na^+ with 100 mM K^+ was used to induce a sustained positive shift in E_m (Fig. 3 C). Thereafter, the introduction of a hyperosmotic sucrose solution was without effect on $[Ca^{2+}]_i$. However, 30 mM caffeine induced a robust increase in $[Ca^{2+}]_i$, indicating that Ca^{2+} remained available for release from the SR.

The cumulative data (Fig. 3 D) show changes in the spatially averaged $[Ca^{2+}]_i$-transient amplitude and E_m after the addition of sucrose or $CaCl_2$ in the presence or absence of 100 μM nifedipine. Also shown is the steady-state E_m after the introduction of a hypoosmotic solution, followed by reintroduction of the control isoosmotic solution. It is apparent that nifedipine markedly inhibits the rise in $[Ca^{2+}]_i$ that occurs after the addition of both hyperosmotic sucrose or $CaCl_2$ solutions.

The role of Cl^- in determining E_m and the effects of cell volume changes

In skeletal muscle, the Cl^- permeability is much higher than that of K^+ and is the primary determinant of the resting E_m (Dulhunty, 1978). Furthermore, there is evidence to suggest that cell volume changes can influence E_m by affecting the activity of the NKCC cotransporter (van Mil et al., 1997). Therefore, further experiments were performed to investigate the role of Cl^- and the NKCC cotransporter in dictating (1) the resting E_m in FDB fibers and (2) the effects of hyperosmotic solutions in FDB fibers.

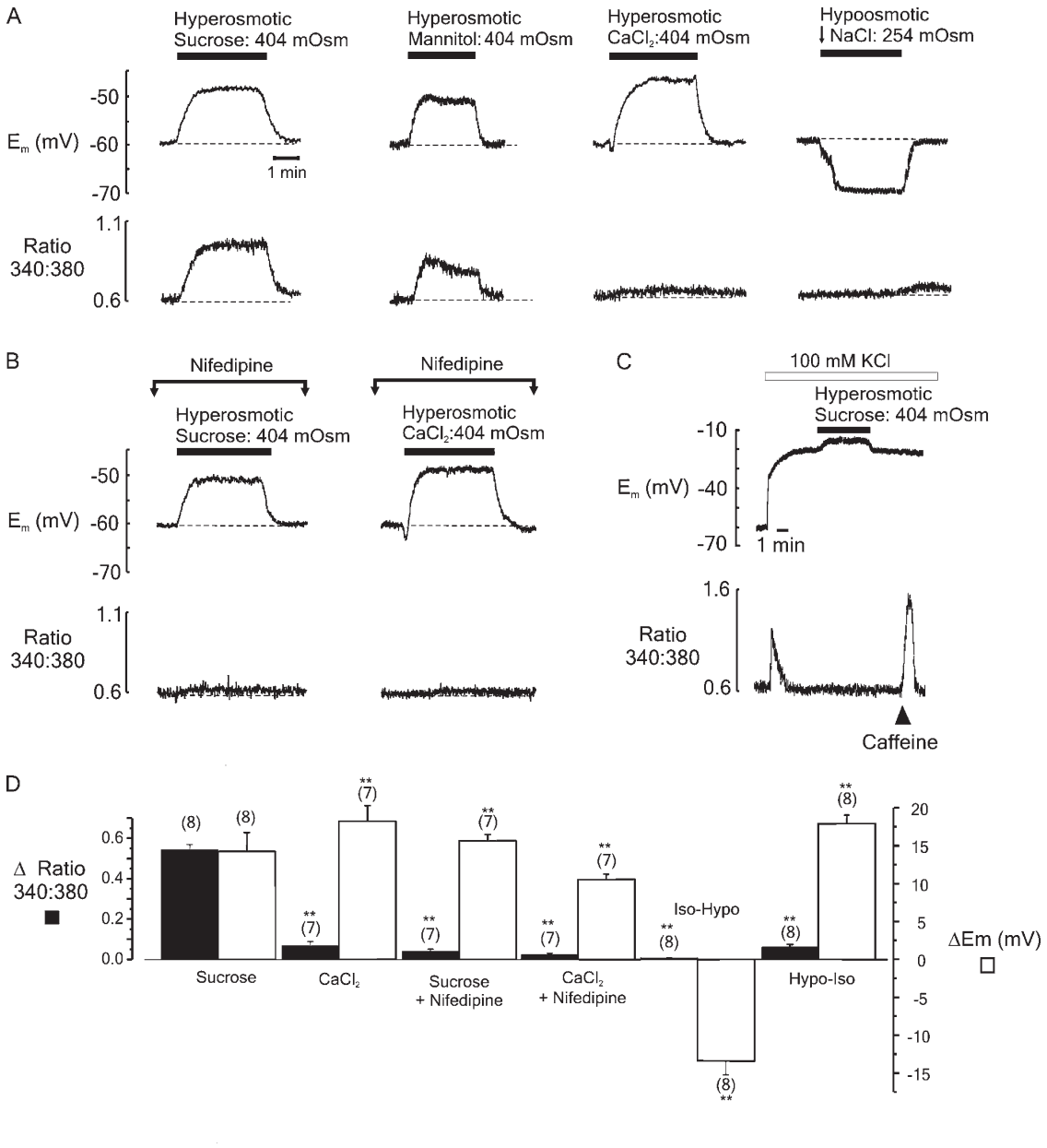

Figure 3. (A) Simultaneous records of E_m (top) and the fura-2 fluorescence ratio (bottom) from fibers equilibrated with an isoosmotic solution before transient exposure to solutions made hyperosmotic (404 mOsm) by the addition of sucrose, mannitol, or $CaCl_2$, or hypoosmotic (254 mOsm) by decreasing [NaCl] (left-right). (B) The effects of hyperosmotic sucrose or $CaCl_2$ solutions on E_m (top) and the fura-2 fluorescence ratio (bottom) in cells exposed to 100 μM nifedipine to inhibit DHPR activation. (C) Substitution of 100 mM Na^+ for K^+ resulted in a sustained depolarization. Thereafter, the introduction of hyperosmotic sucrose solution had no apparent effect on $[Ca^{2+}]_i$, whereas the application of 30 mM caffeine induced a robust $[Ca^{2+}]_i$ transient. (D) Accumulated data showing both the relative change in fluorescence ratio (filled bars) and E_m (open bars) obtained using the protocols shown in A and B. Bars represent the mean (± SEM), and the number of preparations is indicated in parentheses. **, mean values significantly different to the peak values obtained after the introduction of hyperosmotic sucrose ($P < 0.05$).

As shown in Fig. 4 A, the introduction of the Cl^- channel blocker 9-AC resulted in a rapid and reversible hyperpolarization of the cell (to -79.2 ± 3.7 mV; $n = 8$). Some cells (9/17) developed spontaneous action potentials in the presence of 9-AC (Fig. 4 A, right), which is likely due to the reduced stabilizing influence of Cl^- on the resting E_m (Geukes Foppen, 2004). The role of Cl^- was further investigated by reducing the $[Cl^-]$ of the bathing solution. In the example shown in Fig. 4 B (left), the $[Cl^-]$ of the bathing solution was decreased in a stepwise manner from 148 to 10 mM before returning to the control solution. Cl^- depletion resulted in a progressive hyperpolarization, as both $[Cl]_o$ and $[Cl]_i$ decrease. The transient-positive deflection in E_m immediately after

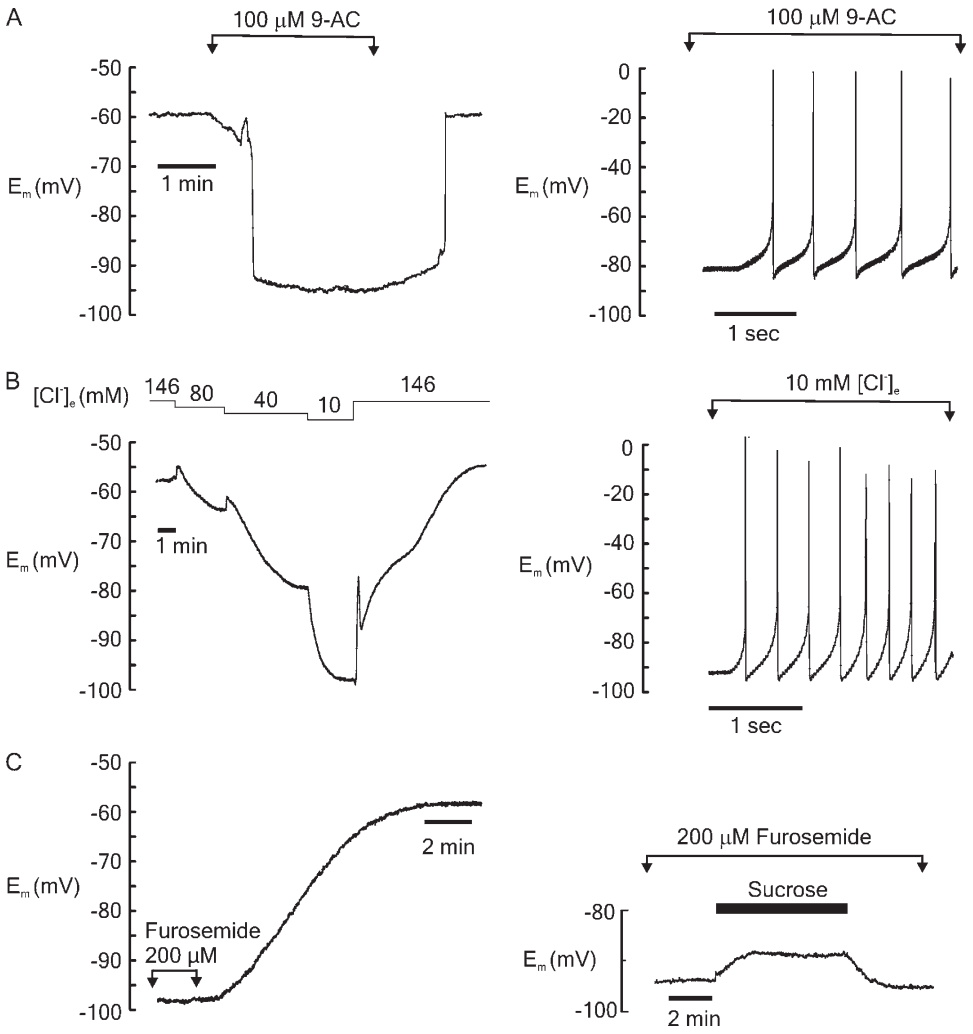

Figure 4. (A) Representative example showing that under isoosmotic conditions, exposure to 9-AC caused a sudden hyperpolarization of E_m by ~30–35 mV (left). This effect was fully reversible on wash-off of 9-AC. In some fibers, the application of 9-AC caused the firing of spontaneous action potentials (right). (B) Graded reduction of $[Cl^-]_e$ caused hyperpolarization of E_m, which fully reversed on return to the control solution (left). Each decrease in $[Cl^-]$ was associated with a small transient hyperpolarization. Again, in some fibers, $[Cl^-]_e$ depletion was associated with spontaneous action potentials (right). (C) Fibers preincubated with the NKCC cotransporter furosemide (200 μM) were typically hyperpolarized relative to control cells, and washoff of the drug was associated with a gradual depolarization of E_m to ~−60 mV (left). In the presence of furosemide, the application of hyperosmotic (404 mOsm) sucrose caused a depolarization of 6 mV (right).

each decrease in $[Cl^-]$ may reflect the fact that an initial decrease in $[Cl]_o$ has a depolarizing effect, which is then overcome by the influence of $[Cl]_i$ depletion (Dulhunty, 1978). On average, E_m decreased to −84.0 ± 2.2 mV ($n = 11$) in the presence of 10 mM $[Cl]_o$, and as with 9-AC, some cells (21/32) developed spontaneous action potentials (Fig. 4 B, right).

The hyperpolarizing effects of 9-AC and reduced Cl^- suggest that (1) the measured resting E_m in FDB fibers reflects the transmembrane Cl^- distribution, and (2) $[Cl^-]_i$ is higher than expected from passive distribution of the ion. Therefore, experiments were performed using the NKCC transport inhibitor furosemide (Gosmanov et al., 2003) to determine whether tonic activation of the transporter is present under control conditions in FDB fibers. As E_m took several minutes to stabilize after the introduction of furosemide (not depicted), fibers were exposed to the drug for 15 min before being impaled. In fibers preincubated with 200 μM furosemide, the resting E_m was −89.2 ± 1.7 mV ($n = 17$). Upon washout of furosemide, E_m decreased to −59.01 ± 1.13 mV ($n = 10$), which was not significantly different from the E_m recorded under control conditions (Fig. 4 C, left). Similar results were obtained with bumetanide, another NKCC transport inhibitor (not depicted).

To investigate the possibility that the membrane depolarization that occurs on the addition of hyperosmotic agents might involve volume-dependent changes in the activity of NKCC, cells were exposed to a hyperosmotic sucrose solution in the presence of 200 μM furosemide (Fig. 4 C, right). In the presence of furosemide, the mean depolarization induced by hyperosmotic sucrose was significantly reduced by 48.3 ± 2.3% ($n = 7$; $P < 0.05$), and the rise in $[Ca^{2+}]$ was decreased by 44.89 ± 1.62% (not depicted).

LCR associated with decreasing cell volume

The inhibitory action of nifedipine suggests that voltage-dependent SR Ca^{2+} release contributes to volume-dependent changes in Ca^{2+} regulation. Therefore, experiments were performed to investigate the role of voltage-dependent Ca^{2+} release in the initiation of LCR, as described recently in FDB fibers under similar conditions (Wang et al., 2005; Martins et al., 2008)

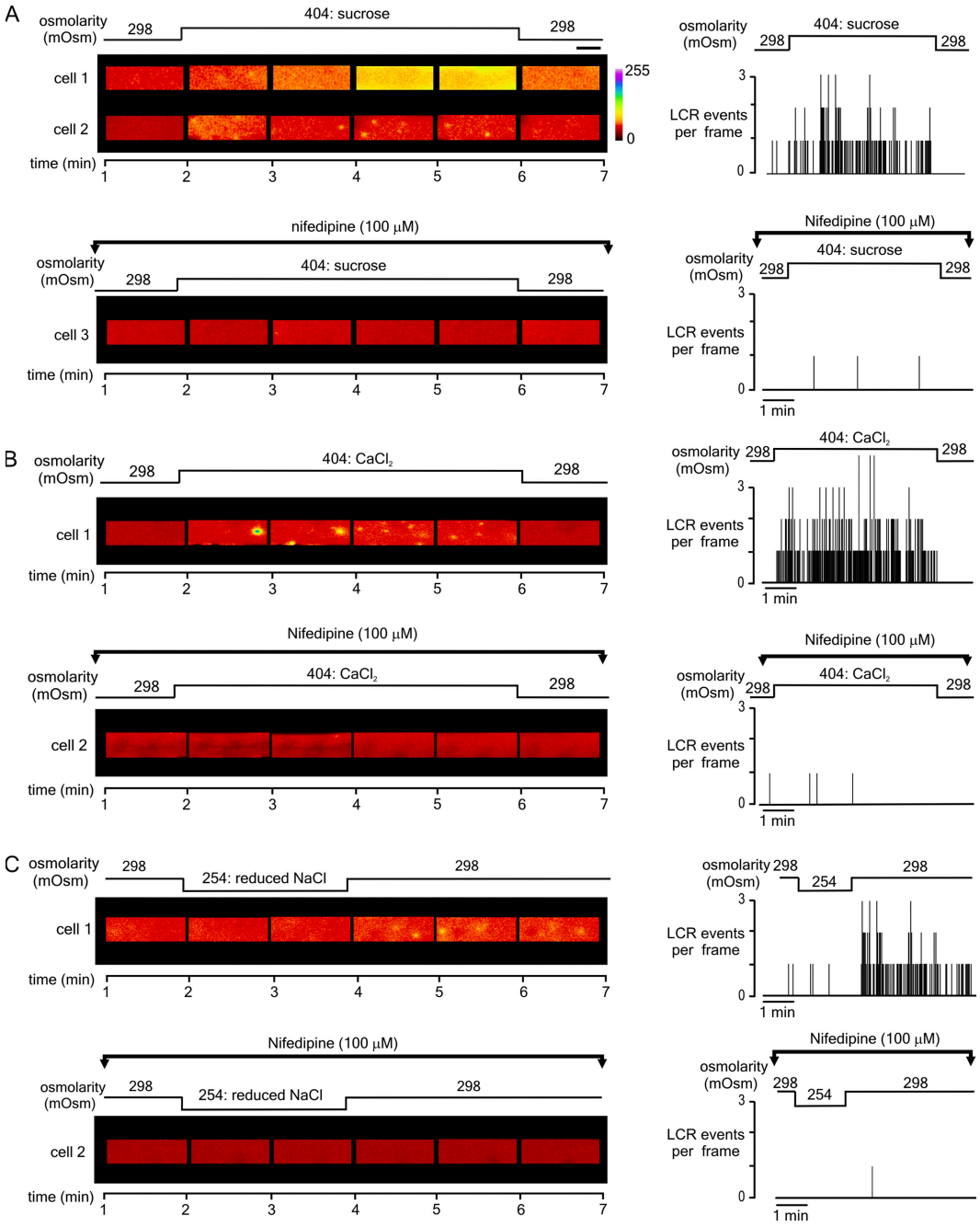

Figure 5. Representative confocal x-y images (1/second) obtained from fluo-4–loaded FDB fibers before, during, and after exposure to solutions of increased or decreased osmolarity. For each cell, the number of LCR events observed per frame throughout the experiment is indicated in the graph on the right. (A) The application of a hyperosmotic sucrose solution was often associated with a marked elevation of $[Ca^{2+}]$, and LCR was difficult to identify (cell 1). However, where the rise in $[Ca^{2+}]$ was less pronounced, individual LCR events were apparent during the application of sucrose (cell 2). Prior exposure to 100 μM nifedipine, to inhibit the DHPR, prevented LCR upon sucrose exposure (cell 3). (B) The introduction of a hyperosmotic $CaCl_2$ solution induced LCR (cell 1), which was markedly inhibited in the presence of nifedipine (cell 2). (C) The application of a hypoosmotic (254 mOsm) solution had no apparent effect on $[Ca^{2+}]_i$. However, returning to the isoosmotic solution precipitated LCR events (cell 1). In the presence of nifedipine, transient exposure to a hypoosmotic solution failed to induce LCR (cell 2). Fibers subject to hypoosmotic Tyrode's exposure were initially exposed to isoosmotic Tyrode for 30 s, and then for 2 min to a hypoosmotic before returning to isoosmotic Tyrode's solution for 4 min. Horizontal bar, 20 μm.

In the experiment shown in Fig. 5, all cells were initially loaded with fluo-4 AM and then superfused with isoosmotic Tyrode's solution. Fig. 5 A shows selected confocal x-y images obtained from two cells before, during, and after exposure to a hyperosmotic sucrose solution (top left). Consistent with the spatially averaged $[Ca^{2+}]_i$ measurements (Fig. 2), the introduction of hyperosmotic sucrose solution typically (six out of

seven cells) induced a rapid increase in global $[Ca^{2+}]_i$ (cell 1). Against this background of elevated $[Ca^{2+}]_i$, LCR was often difficult to identify. However, where the rise in $[Ca^{2+}]_i$ was relatively small, LCR was clearly present (cell 2). Importantly, in the presence of nifedipine (cell 3), neither a rise in global $[Ca^{2+}]_i$ nor an increase in LCR frequency was apparent after the introduction of hyperosmotic sucrose solution. Summary data from cells 2 and 3, showing the number of LCR events per frame throughout both experiments (Fig. 5 A, right), emphasize that (1) when present, LCR primarily occurred during exposure to the hyperosmotic solution, and (2) the triggering of LCR by hyperosmotic sucrose solution is essentially abolished in the presence of nifedipine.

As shown in Fig. 5 B, the introduction of solutions made hyperosmotic by the addition of $CaCl_2$ induced LCR, but without a large rise in global $[Ca^{2+}]_i$ (cell 1). However, in the presence of nifedipine, LCR frequency was unchanged after the introduction of the hyperosmotic $CaCl_2$ solution (cell 2). Similar results were obtained in six other cells exposed to hyperosmotic $CaCl_2$ solution and seven other cells exposed to hyperosmotic $CaCl_2$ in the presence of nifedipine (not depicted).

In Fig. 5 C, transient exposure to hypoosmotic Tyrode's solution resulted in the generation of LCR (cell 1). Again, this increase in spark frequency was markedly inhibited by nifedipine (cell 2). The summary data (Fig. 5 C, right) illustrate that (1) LCR occurs only at a very low frequency before or during exposure to the hypoosmotic solution, (2) LCR only becomes apparent on return to the isoosmotic solution, and (3) LCR is sustained for at least 4 min. Similar results were obtained in seven other cells transiently exposed to the hypoosmotic solution and in six other cells transiently exposed to the hypoosmotic Tyrode's solution in the presence of nifedipine. Under all conditions, LCR events tended to occur at highest frequency close to the cell periphery, as reported previously (Wang et al., 2005).

Further experiments were performed using line-scan (x-t) confocal imaging to investigate the spatial and temporal properties of LCR events in more detail. Fig. 6 A shows a typical x-t image and associated line profiles obtained after an increase in the solution osmolarity from 298 to 404 mOsm produced by the addition of $CaCl_2$ (left) or sucrose (right). A marked heterogeneity of durations is apparent, ranging from very brief Ca^{2+} sparks to much longer events lasting several hundred milliseconds, previously referred to as "bursts" (Wang et al., 2005). One notable feature is that where LCR occurs repeatedly from a given Ca^{2+} release site, the events tend to have very similar characteristics. As expected, some variation in amplitude is apparent among Ca^{2+} release sites, although this is partly due to events that originate above or below the confocal plane. The cumulative data shows characteristic histograms of LCR amplitudes (Fig. 6 B, left) and widths (right), which are unimodal, with the amplitude distribution skewed to the left and full width half duration values conforming to an approximately symmetrical Gaussian distribution.

The mean amplitudes of the LCR events in response to hyperosmotic sucrose (1.32 ± 0.01 F/F_o; $n = 312$) or transient hypoosmotic exposure (1.33 ± 0.01 F/F_o; $n = 307$; $P > 0.05$) were not significantly different, although both were significantly smaller than the mean amplitude of events induced by hyperosmotic $CaCl_2$ (1.57 ± 0.01 F/F_o; $n = 803$; $P < 0.05$). The mean width (full width half maximum) of LCR events in response to hyperosmotic sucrose, transient hypoosmotic exposure, and hyperosmotic $CaCl_2$ solution was 2.72 ± 0.06 ($n = 321$), 3.15 ± 0.1 ($n = 307$), and 2.9 ± 0.03 μm ($n = 803$), respectively, and these values all differed significantly from each other ($P < 0.05$).

Interestingly, the distribution of LCR durations was bimodal, suggesting that Ca^{2+} sparks and Ca^{2+} bursts represent two distinct populations of events, with the latter exhibiting a markedly greater variance. This bimodal distribution is most apparent with events triggered by hyperosmotic $CaCl_2$, where the total number of events collected was greatest, and the curve shown (Fig. 6 C, broken line) is fitted to these values only. The duration (full duration half maximum [FDHM]) mode peaks occurred at 30.5 and 177.4 ms. Although less clearly defined, histograms of LCR durations triggered by hyperosmotic sucrose or transient exposure to hypoosmotic media also appear bimodal (Fig. 6 C, inset).

Cumulative data showing the relative frequencies of LCR events during the peak of the responses to hyperosmotic sucrose, hyperosmotic $CaCl_2$, or transient exposure to a hypoosmotic solution are given in Fig. 7. Also shown are the values obtained when the same protocols were performed in the presence of nifedipine. In the presence of nifedipine, the peak LCR frequencies were not significantly different to the basal level observed in the control (isoosmotic) solution ($P > 0.05$).

DISCUSSION

Previous studies on isolated skeletal muscle have sought to establish the physiological or pathological consequences of cell volume changes by altering the osmolarity of solutions bathing isolated fibers (Clausen et al., 1979; Bruton, 1989; Chawla et al., 2001; Wang et al., 2005; Weisleder et al., 2006; Martins et al., 2008; Weisleder and Ma, 2008; Teichmann et al., 2008). However, markedly different effects on $[Ca^{2+}]_i$ were reported depending on the osmotic agent used. In the present study, we show that these disparate results can be explained by volume-dependent changes in resting E_m and consequent effects on RYR1 activation.

Changes in $[Ca^{2+}]_i$ induced by osmotic agents

Exposure to hyperosmotic sucrose solutions caused a rapid increase in spatially averaged $[Ca^{2+}]_i$, which was

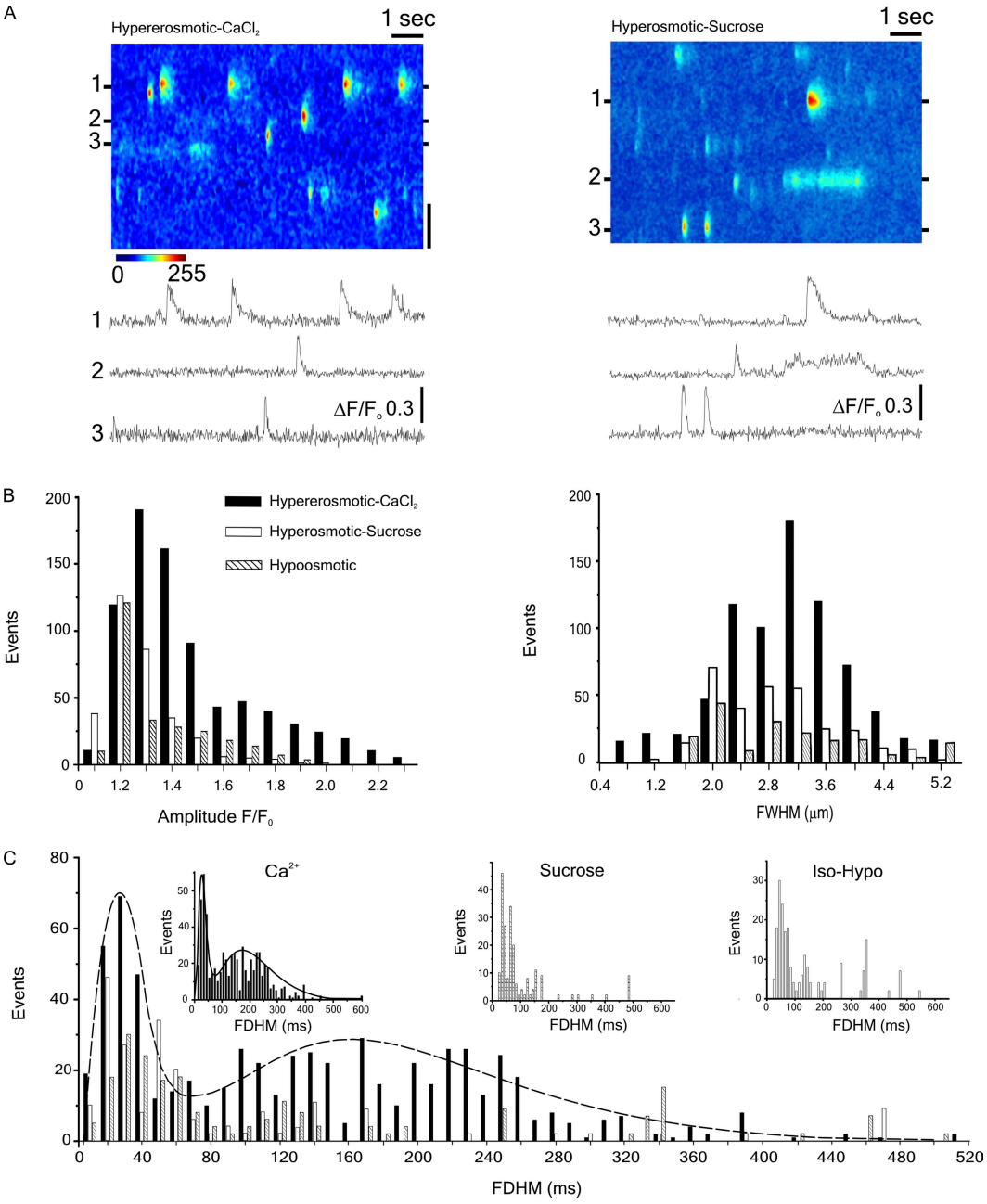

Figure 6. (A) Line-scan image and associated line profiles obtained after an increase in solution osmolarity from 298 to 404 mOsm by the addition of $CaCl_2$ (left) or sucrose solution (right). (B) Histograms of LCR amplitudes (F/F_o) and widths (FWHM) after the introduction of hyperosmotic (404 mOsm) $CaCl_2$ or sucrose solutions, or transient exposure to a hypoosmotic (254 mOsm) solution. (C) Histogram showing bimodal distribution of LCR durations (FDHM). Curve fitted to data obtained after the introduction of hyperosmotic $CaCl_2$. Insets show individual datasets. Vertical bar, 2 μm.

strongly inhibited by tetracaine (Fig. 2). This suggests that the decrease in cell volume induced by a hyperosmotic sugar solutions leads to activation of RYR1 and a consequent rise in $[Ca^{2+}]_i$. This large increase in $[Ca^{2+}]_i$ can explain early observations that hyperosmotic sucrose solutions induce contractures in rat skeletal muscle (Clausen et al., 1979; Bruton, 1989).

The increase in mean $[Ca^{2+}]_i$ induced by solutions made hyperosmotic by the addition of divalent ions was much smaller than that which occurred with sugars (Fig. 2), despite a comparable change in cell volume (Fig. 1). Indeed, the small increase in the average $[Ca^{2+}]_i$ after the introduction of hyperosmotic $CaCl_2$ solution (Fig. 2 B) likely reflects the presence of LCR events apparent only in confocal images (e.g., Fig. 5). The absence of a larger global rise in $[Ca^{2+}]$ might be explained if increased levels of divalent ions in the extracellular fluid inhibit the process, leading to SR Ca^{2+} release (see below).

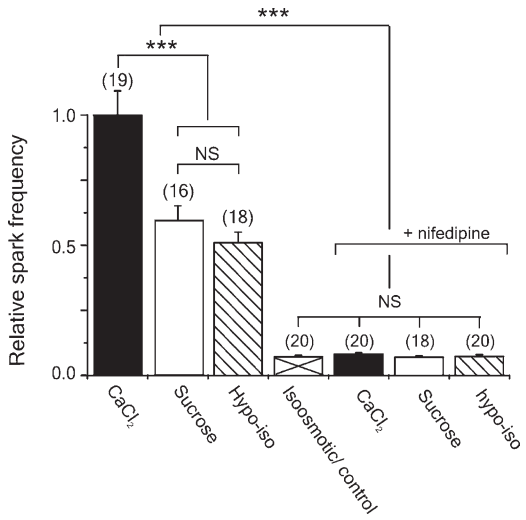

Figure 7. Cumulative data showing the relative frequencies of LCR events during the peak of the responses to hyperosmotic sucrose, hyperosmotic $CaCl_2$, or after transient exposure to a hypoosmotic solution in the absence or presence of nifedipine. ***, statistically significant differences ($P < 0.01$). In the presence of nifedipine, the peak LCR frequencies were not significantly different to the basal frequency observed in the control (isoosmotic) solution ($P > 0.05$).

In some fibers, LCR was difficult to detect after the introduction of hyperosmotic sugar solutions. However, LCR was clearly apparent in fibers that exhibited relatively small rises in the average $[Ca^{2+}]_i$ after the introduction of sucrose (Fig. 5 A). This suggests that LCR is triggered by hyperosmotic sugar solutions but that the events are often obscured by the pronounced increase in the average $[Ca^{2+}]_i$ and/or abolished by depletion of SR Ca^{2+}.

As reported previously (Wang et al., 2005), LCR could be induced by transient exposure to hypoosmotic Tyrode's solution (Fig. 5 C), and the appearance of LCR coincided with the decrease in cell volume that followed the reintroduction of the control isoosmotic solution. A robust LCR response also occurred on exposure to a hyperosmotic $CaCl_2$ solution (Fig. 5, A and B), again suggesting that the initiation of LCR is associated with decreasing cell volume, and that a preceding period of cell swelling is not required.

Resting E_m in FDB fibers

In the present study, the mean resting E_m was -60.1 ± 2.91 ($n = 67$). This is consistent with other published E_m values obtained in FDB fibers, which range from -60 to -67 mV (Bekoff and Betz, 1977a,b; Westerblad and Allen, 1996). In control experiments, similar values were measured from the surface fibers of freshly dissected whole FDB muscles superfused with Tyrode's solution, suggesting that cell isolation has relatively little influence on E_m under these conditions (see Materials and methods). Another recent study addressing the effects of osmotic shock in mouse interossei muscle found the mean resting E_m to be -65 mV recorded in situ (Teichmann et al., 2008). These findings suggest that the relatively low resting E_m in FDB fibers might reflect some aspect of physiological specialization rather than cell damage. This possibility is supported by observations that the resting E_m in FDB fibers is consistently 10–15 mV more positive than in extensor digitorum longus or soleus muscles, recorded under identical conditions (unpublished data). Although the functional significance of these variations in resting E_m is uncertain, previous work suggests that the physiological SR Ca^{2+} release in response to an action potential is little affected as long as the resting E_m remains more negative than -60 mV (Dutka and Lamb, 2007).

In skeletal muscle, the resting Cl^- permeability is approximately four times higher than that of K^+ (Bryant and Morales-Aguilera, 1971; Palade and Barchi, 1977; Dulhunty, 1979) and therefore the major determinant of the resting E_m. Based on typical values for the relative permeabilities of Cl^-, K^+, and Na^+ (400:100:1, respectively) and transmembrane ion concentrations ($[Cl^-]_i$ 4.1 mM, $[K^+]_i$ 150 mM, $[Na^+]_i$ 12 mM, $[Cl^-]_o$ 116 mM, $[K^+]_o$ 4.5 mM, and $[Na^+]_o$ 145 mM), E_m would be expected to be around -83 mV (Goldman equation; 22°C). The more positive resting E_m typically measured in skeletal muscle (and FDB fibers in particular) might reflect active Cl^- transport, which increases $[Cl]_i$ to a level above that expected from passive distribution (Dulhunty, 1978; van Mil et al., 1997; Geukes Foppen, 2004). In the present study, several findings are consistent with this suggestion: (1) decreasing the $[Cl^-]_o$ to 10 mM caused a sustained hyperpolarization of ~25 mV, and (2) the Cl^- channel blocker 9-AC or the NKCC inhibitor furosemide induced membrane hyperpolarizations of 18.9 ± 2.3 ($n = 8$) and 26.4 ± 2.5 mV ($n = 17$), respectively (Fig. 4).

Furosemide (or bumetanide; not depicted) markedly inhibited the depolarization associated with decreasing cell volume (Fig. 4). This suggests that the NKCC transporter provides an important link between cell volume and the observed changes in E_m. The fact that neither drug completely abolished the positive shift in E_m after exposure to hyperosmotic solutions may reflect incomplete inhibition of NKCC or the involvement of other factors that influence the electrochemical equilibrium (e.g., concentration of Cl^- within the cytosol after the outward movement of water).

Cell volume, E_m, and SR Ca^{2+} release

This is the first study to demonstrate that DHPR inhibition abolishes LCR triggered by hyperosmotic solutions or transient exposure to a hypoosmotic solution (Figs. 5 and 7). SR Ca^{2+} efflux was also abolished by tonic depolarization of the sarcolemma induced by increasing $[K^+]_o$ (Fig. 3). These data suggest that the positive shift

in E_m that occurs on decreasing cell volume leads to submaximal DHPR activation, which in turn triggers Ca^{2+} efflux via RYR1.

As summarized in Fig. 8, a causal relationship between decreasing cell volume, membrane depolarization, and RYR1 activation can explain the differing properties of SR Ca^{2+} release induced by sugars or divalent ions. From a resting E_m of −60 mV, we propose that the depolarization associated with exposure to hyperosmotic sugar solutions activates a proportion of the available DHPRs, leading to robust activation of RYR1 and a rise in the spatially averaged $[Ca^{2+}]_i$. The global SR Ca^{2+} release observed under these conditions is consistent with findings that voltage-dependent activation of DHPRs increases steeply as E_m becomes more positive than −50 mV (Ursu et al., 2004).

On the introduction of solutions made hyperosmotic by the addition of $CaCl_2$ or $MgCl_2$, the same decrease in cell volume resulted in a much smaller release of Ca^{2+} from the SR (Figs. 1 and 2). This may be explained by studies showing that the screening of surface charges by divalent ions reduces the responsiveness of voltage-sensitive channels by offsetting the local potential difference across the protein (Green and Andersen, 1991). However, the unsuitability of using 50 mM $CaCl_2$ in studies investigating $[Ca^{2+}]_i$ dynamics (Wang et al., 2005) has already been pointed out (Teichmann et al., 2008).

The SR Ca^{2+} release that occurs after a transient decrease in osmolarity (Fig. 2 A) is likely related to the fact that E_m is around −60 mV under control conditions, causing sustained inactivation of a small proportion of DHPRs (Ursu et al., 2004). As cell volume increases during hypoosmotic exposure, the resulting hyperpolarization will lead to "re-priming" of these DHPRs. Thereafter, on return to the isoosmotic solution, the depolarization that accompanies restoration of cell volume will induce activation of these DHPRs, resulting in LCR. This proposed sequence of events is supported by the fact that nifedipine inhibits the induction of LCR on the reintroduction of isoosmotic media (Fig. 5).

Bimodal distribution of Ca^{2+} spark durations

This is the first study to describe a bimodal distribution of LCR durations induced by osmotic stress (Fig. 6). In a recent study in mouse interossei muscle, LCR durations were presented as an apparently unimodal distribution (Teichmann et al., 2008). However, these authors did not present cumulative data for LCR events with FDHM values >45 ms (Teichmann et al., 2008); therefore, the second mode would not have been apparent. The only other study to present cumulative data on LCR induced by osmotic stress also reported a unimodal FDHM distribution in mouse FDB fibers (Weisleder et al., 2007). In this case, the absence of a bimodal FDHM distribution might reflect a species difference, although this seems unlikely because we have observed a similar bimodal distribution in mouse FDB fibers (not depicted). An alternative possibility is that the chosen bin size of data presented in histogram format may have obscured the transient decline in event frequency between the mode peaks.

A bimodal distribution suggests the presence of two functionally distinct populations of Ca^{2+} release sites.

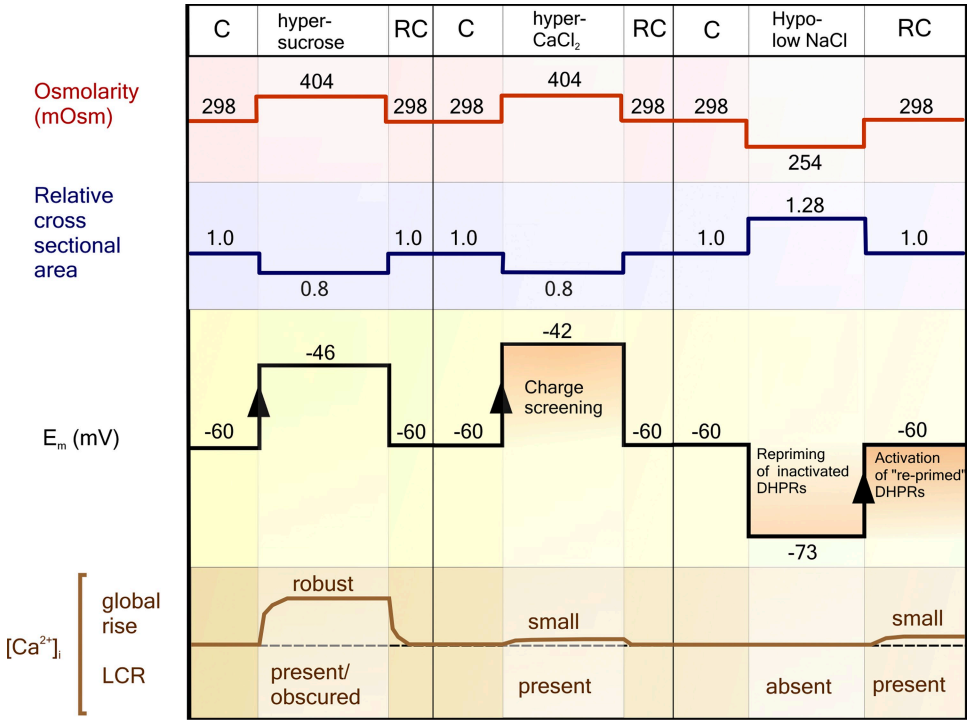

Figure 8. Diagram summarizing the observed effects of hyperosmotic and hypoosmotic solutions on E_m and SR Ca^{2+} release. Also shown are the proposed effects of (1) charge screening during exposure to hyperosmotic $CaCl_2$ solutions and (2) transient hyperpolarization from a resting E_m of ∼−60 mV on DHPR function. C, control solution; RC, re-control.

The first population is comprised of relativity brief "typical" Ca^{2+} sparks. The second population has greater variance and comprises events of much greater duration previously termed Ca^{2+} bursts (Wang et al., 2005). It should be noted, however, that despite the marked variation in event durations overall, the temporal and spatial characteristics of LCR events at individual Ca^{2+} release sites were highly consistent (Fig. 6 A).

One possible explanation for an apparently distinct population of prolonged LCR events is the involvement of the RYR3 isoform, which is expressed at a low level in adult muscle but known to facilitate Ca^{2+}-induced Ca^{2+} release and voltage-dependent LCR (Pouvreau et al., 2007). However, this is unlikely because Ca^{2+} bursts have been demonstrated after ablation of RYR3 (Weisleder et al., 2007). An alternative possibility is that prolonged LCR events reflect differences in the structures that couple mechanical deformation of the sarcolemma at the cell periphery (Teichmann et al., 2008) to RYR1 activation (see below).

Relationship to previous studies

The present study links early work describing the role of Cl^- in dictating the resting E_m in skeletal muscle (Dulhunty, 1978) to the identification of NKCC in skeletal muscle (van Mil et al., 1997) and recent findings that LCR can be triggered by cell volume changes (Wang et al., 2005; Weisleder et al., 2006; Martins et al., 2008). Given the profound inhibitory effects of nifedipine or sustained membrane depolarization shown in the present study, it is reasonable to conclude that DHPR activation is necessary for volume-dependent SR Ca^{2+} release, whether global or local. This is a potentially important mechanism to have been identified because of the known changes in muscle fiber volume that occur in response to exercise and the alterations in $[Ca^{2+}]_i$ signaling associated with aging or disease (Wang et al., 2005; Teichmann et al., 2008; Weisleder and Ma, 2008).

This primary role of DHPR activation in the initiation of LCR events during osmotic stress does not exclude other proposed influences on the SR Ca^{2+} release mechanism; indeed, in the absence of an accompanying volume change, mammalian skeletal muscle responds to a small depolarization with events that appear similar to "lone embers" first described in permeabilized cells (Csernoch et al., 2004). These events are smaller in amplitude than Ca^{2+} sparks but of much longer duration. This suggests that some other volume-dependent factor alters the response to depolarization, resulting in a more heterogeneous population of LCR events that includes Ca^{2+} sparks. As proposed in earlier studies, this might involve mechanical deformation of the membrane (Teichmann et al., 2008), structural changes in the triadic junction (Wang et al., 2005), or increased reactive oxygen species production (Isaeva et al., 2005; Martins et al., 2008).

The change in $[Ca^{2+}]_i$ signaling in response to osmotic stress is more pronounced in MDX fibers, leading to the suggestion that LCR may serve as a dystrophic signal (Wang et al., 2005). Furthermore, a recent study by Teichmann et al. (2008) showed that (1) the enhanced response to osmotic stress in MDX mice could be reversed by expression of mini-dystrophin, and (2) Ca^{2+} influx via stretch-activated Ca^{2+} channels (SACs) partially amplified the effect of osmotic stress in MDX muscle. A model was proposed in which dystrophin provides a stabilizing structural link between sarcolemmal SACs and the DHPR-RYR1 "inhibitory loop." It was suggested that, in the absence of dystrophin, (1) osmotic stress and consequent membrane deformation has a greater effect on SACs, and (2) the DHPR exerts a reduced inhibitory effect on RYR1. This proposed mechanical transduction mechanism might be of relevance to the current findings because reduced inhibition of RYR1 via the DHPR inhibitory loop could amplify the effect of a submaximal membrane depolarization.

Our observation of a depolarization on the introduction of hyperosmotic solutions differs from that of Teichmann et al. (2008), who observed a slight hyperpolarization. Although the reasons for this discrepancy are not clear, there are several differences in the experimental conditions. First, Teichmann et al. used a much higher level of sucrose (300 mM as opposed to 120 mM). Second, E_m was measured from fibers in situ, but not during blood perfusion, raising questions about the metabolic status of the cells. Third, E_m was measured from different populations of fibers exposed to each osmotic solution, which makes it less easy to resolve small changes in E_m. The hyperpolarization reported by Teichmann et al. (2008) is also at variance with other studies reporting a depolarization linked to changes in NKCC activity (van Mil et al., 1997; Geukes Foppen, 2004).

Summary

Hyperosmotic and hypoosmotic solutions induce corresponding positive and negative shifts in E_m, respectively, which in part reflect volume-dependent changes in the activity of NKCC and consequent effects on $[Cl^-]_i$. These changes in E_m act via the DHPR to induce either global SR Ca^{2+} release (on the introduction of hyperosmotic sugar solutions) or LCR (after transient exposure to hypoosmotic media or the introduction of solutions made hyperosmotic by the addition of divalent ions). The less pronounced Ca^{2+} release observed in the presence of divalent ions is consistent with the expected effects of charge screening. This work provides valuable mechanistic information regarding the initiation of LCR reported to occur as a consequence of intense exercise or disease.

Financial support of the Medical Research Council UK and the Wellcome Trust is acknowledged. J.D. Pickering was funded by a University of Leeds Scholarship.

Edward N. Pugh Jr. served as editor.

Submitted: 6 January 2009
Accepted: 10 April 2009

REFERENCES

Bekoff, A., and W. Betz. 1977a. Properties of isolated adult rat muscle fibres maintained in tissue culture. *J. Physiol.* 271:537–547.

Bekoff, A., and W.J. Betz. 1977b. Physiological properties of dissociated muscle fibres obtained from innervated and denervated adult rat muscle. *J. Physiol.* 271:25–40.

Bruton, J.D. 1989. Role of chloride in hypertonicity-induced contractures of rat soleus muscle. *Q. J. Exp. Physiol.* 74:565–567.

Bryant, S.H., and A. Morales-Aguilera. 1971. Chloride conductance in normal and myotonic muscle fibres and the action of monocarboxylic aromatic acids. *J. Physiol.* 219:367–383.

Chawla, S., J.N. Skepper, A.R. Hockaday, and C.L. Huang. 2001. Calcium waves induced by hypertonic solutions in intact frog skeletal muscle fibres. *J. Physiol.* 536:351–359.

Clausen, T., A.B. Dahl-Hansen, and J. Elbrink. 1979. The effect of hyperosmolarity and insulin on resting tension and calcium fluxes in rat soleus muscle. *J. Physiol.* 292:505–526.

Csernoch, L., J. Zhou, M.D. Stern, G. Brum, and E. Rios. 2004. The elementary events of Ca^{2+} release elicited by membrane depolarization in mammalian muscle. *J. Physiol.* 557:43–58.

Dulhunty, A.F. 1978. The dependence of membrane potential on extracellular chloride concentration in mammalian skeletal muscle fibres. *J. Physiol.* 276:67–82.

Dulhunty, A.F. 1979. Distribution of potassium and chloride permeability over the surface and T-tubule membranes of mammalian skeletal muscle. *J. Membr. Biol.* 45:293–310.

Dutka, T.L., and G.D. Lamb. 2007. Transverse tubular system depolarization reduces tetanic force in rat skeletal muscle fibers by impairing action potential repriming. *Am. J. Physiol. Cell Physiol.* 292:C2112–C2121.

Ferenczi, E.A., J.A. Fraser, S. Chawla, J.N. Skepper, C.J. Schwiening, and C.L. Huang. 2004. Membrane potential stabilization in amphibian skeletal muscle fibres in hypertonic solutions. *J. Physiol.* 555:423–438.

Geukes Foppen, R.J. 2004. In skeletal muscle the relaxation of the resting membrane potential induced by K^+ permeability changes depends on Cl(-) transport. *Pflugers Arch.* 447:416–425.

Gosmanov, A.R., M.I. Lindinger, and D.B. Thomason. 2003. Riding the tides: K+ concentration and volume regulation by muscle Na+-K+-2Cl- cotransport activity. *News Physiol. Sci.* 18:196–200.

Green, W.N., and O.S. Andersen. 1991. Surface charges and ion channel function. *Annu. Rev. Physiol.* 53:341–359.

Hattori, T., and P.L. Wang. 2006. Involvement of Na(+)-K(+)-2Cl(-) cotransporters in hypertonicity-induced rise in intracellular calcium concentration. *Int. J. Neurosci.* 116:1501–1507.

Isaeva, E.V., V.M. Shkryl, and N. Shirokova. 2005. Mitochondrial redox state and Ca^{2+} sparks in permeabilized mammalian skeletal muscle. *J. Physiol.* 565:855–872.

Lannergren, J., H. Westerblad, and J.D. Bruton. 2002. Dynamic vacuolation in skeletal muscle fibres after fatigue. *Cell Biol. Int.* 26:911–920.

Martins, A.S., V.M. Shkryl, M.C. Nowycky, and N. Shirokova. 2008. Reactive oxygen species contribute to Ca^{2+} signals produced by osmotic stress in mouse skeletal muscle fibres. *J. Physiol.* 586:197–210.

Nagesser, A.S., W.J. van der Laarse, and G. Elzinga. 1992. Metabolic changes with fatigue in different types of single muscle fibres of Xenopus laevis. *J. Physiol.* 448:511–523.

Palade, P.T., and R.L. Barchi. 1977. Characteristics of the chloride conductance in muscle fibers of the rat diaphragm. *J. Gen. Physiol.* 69:325–342.

Peeze Binkhorst, F.M., D.W. Slaaf, H. Kuipers, G.J. Tangelder, and R.S. Reneman. 1990. Exercise-induced swelling of rat soleus muscle: its relationship with intramuscular pressure. *J. Appl. Physiol.* 69:67–73.

Picht, E., A.V. Zima, L.A. Blatter, and D.M. Bers. 2007. SparkMaster: automated calcium spark analysis with ImageJ. *Am. J. Physiol. Cell Physiol.* 293:C1073–C1081.

Pouvreau, S., L. Royer, J. Yi, G. Brum, G. Meissner, E. Rios, and J. Zhou. 2007. Ca^{2+} sparks operated by membrane depolarization require isoform 3 ryanodine receptor channels in skeletal muscle. *Proc. Natl. Acad. Sci. USA.* 104:5235–5240.

Raja, M.K., G.H. Raymer, G.R. Moran, G. Marsh, and R.T. Thompson. 2006. Changes in tissue water content measured with multiple-frequency bioimpedance and metabolism measured with 31P-MRS during progressive forearm exercise. *J. Appl. Physiol.* 101:1070–1075.

Sejersted, O.M., and G. Sjogaard. 2000. Dynamics and consequences of potassium shifts in skeletal muscle and heart during exercise. *Physiol. Rev.* 80:1411–1481.

Sjogaard, G., R.P. Adams, and B. Saltin. 1985. Water and ion shifts in skeletal muscle of humans with intense dynamic knee extension. *Am. J. Physiol.* 248:R190–R196.

Teichmann, M.D., F.V. Wegner, R.H. Fink, J.S. Chamberlain, B.S. Launikonis, B. Martinac, and O. Friedrich. 2008. Inhibitory control over Ca^{2+} sparks via mechanosensitive channels is disrupted in dystrophin deficient muscle but restored by mini-dystrophin expression. *PLoS One.* 3:e3644.

Ursu, D., R.P. Schuhmeier, M. Freichel, V. Flockerzi, and W. Melzer. 2004. Altered inactivation of Ca^{2+} current and Ca^{2+} release in mouse muscle fibers deficient in the DHP receptor γ_1 subunit. *J. Gen. Physiol.* 124:605–618.

van Mil, H.G., R.J. Geukes Foppen, and v.H. Siegenbeek. 1997. The influence of bumetanide on the membrane potential of mouse skeletal muscle cells in isotonic and hypertonic media. *Br. J. Pharmacol.* 120:39–44.

Wang, K., and R. Wondergem. 1992. Mouse hepatocyte membrane potential and chloride activity during osmotic stress. *Am. J. Physiol.* 263:G566–G572.

Wang, X., N. Weisleder, C. Collet, J. Zhou, Y. Chu, Y. Hirata, X. Zhao, Z. Pan, M. Brotto, H. Cheng, and J. Ma. 2005. Uncontrolled calcium sparks act as a dystrophic signal for mammalian skeletal muscle. *Nat. Cell Biol.* 7:525–530.

Watson, P.D., R.P. Garner, and D.S. Ward. 1993. Water uptake in stimulated cat skeletal muscle. *Am. J. Physiol.* 264:R790–R796.

Weisleder, N., and J. Ma. 2006. Ca^{2+} sparks as a plastic signal for skeletal muscle health, aging, and dystrophy. *Acta Pharmacol. Sin.* 27:791–798.

Weisleder, N., and J. Ma. 2008. Altered Ca^{2+} sparks in aging skeletal and cardiac muscle. *Ageing Res. Rev.* 7:177–188.

Weisleder, N., M. Brotto, S. Komazaki, Z. Pan, X. Zhao, T. Nosek, J. Parness, H. Takeshima, and J. Ma. 2006. Muscle aging is associated with compromised Ca^{2+} spark signaling and segregated intracellular Ca^{2+} release. *J. Cell Biol.* 174:639–645.

Weisleder, N., C. Ferrante, Y. Hirata, C. Collet, Y. Chu, H. Cheng, H. Takeshima, and J. Ma. 2007. Systemic ablation of RyR3 alters Ca^{2+} spark signaling in adult skeletal muscle. *Cell Calcium.* 42:548–555.

Westerblad, H., and D.G. Allen. 1996. The effects of intracellular injections of phosphate on intracellular calcium and force in single fibers of mouse skeletal-muscle. *Pflugers Arch.* 431:964–970.